Cell Reports
Methods

Resource

Differential performance of strategies for single-cell whole-genome amplification

Graphical abstract

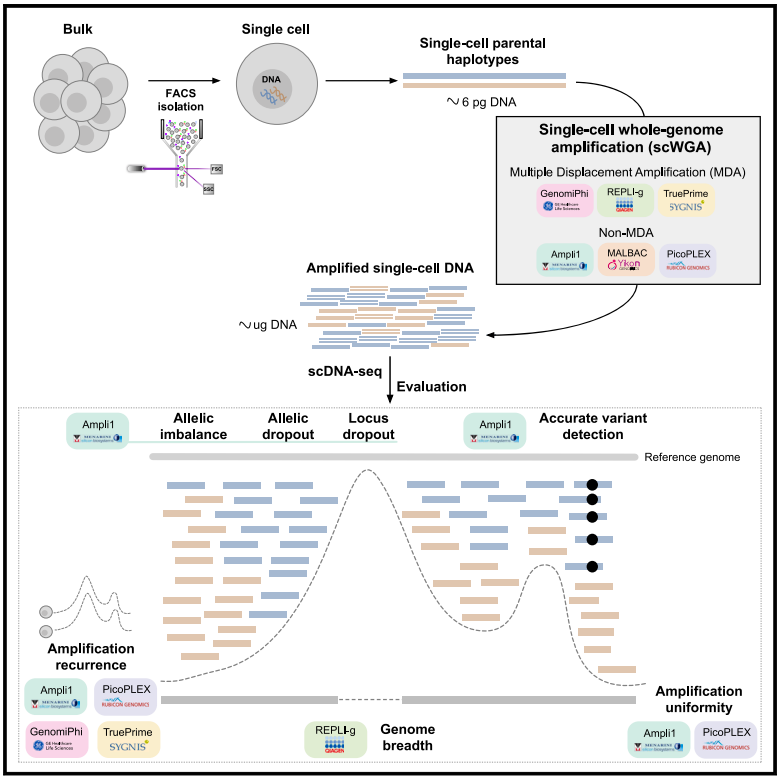

Highlights

- No scWGA method is entirely superior; method choice should be based on study goals
- Non-MDA scWGA methods display a more uniform and reproducible amplification
- Ampli1 shows the lowest allele dropout rate and one of the smaller false positive rates
- REPLI-g provides the longest amplicons and the highest genome breadth

Authors

Nuria Estévez-Gómez, Tamara Prieto, Laura Tomás, ..., Holger Heyn, Sonia Prado-López, David Posada

Correspondence

sonia.prado.gz@gmail.com (S.P.-L.), dposada@uvigo.es (D.P.)

In brief

Estévez-Gómez et al. evaluate the performance of six single-cell whole-genome amplification (scWGA) methods, focusing on important metrics such as genome coverage, amplification error, allelic dropout, and variant-calling accuracy. Their findings provide a useful guide to help researchers choose the most appropriate scWGA strategy for single-cell DNA experiments.

Estévez-Gómez et al., 2025, Cell Reports Methods *5*, 101025
April 21, 2025
https://doi.org/10.1016/j.crmeth.2025.101025

CellPress

Cell Reports Methods

CellPress
OPEN ACCESS

Resource

Differential performance of strategies for single-cell whole-genome amplification

Nuria Estévez-Gómez,[1,2,10] Tamara Prieto,[1,2,6,10] Laura Tomás,[1,2] Pilar Alvariño,[1,2,7] Amy Guillaumet-Adkins,[3,4,8] Holger Heyn,[3,4] Sonia Prado-López,[1,2,9,*] and David Posada[1,2,5,11,*]

[1]CINBIO, Universidade de Vigo, 36310 Vigo, Spain
[2]Galicia Sur Health Research Institute (IIS Galicia Sur), SERGAS-UVIGO, 36312 Vigo, Spain
[3]Centro Nacional de Análisis Genómico (CNAG), 08028 Barcelona, Spain
[4]Universitat de Barcelona (UB), Barcelona, Spain
[5]Department of Biochemistry, Genetics, and Immunology, Universidade de Vigo, 36310 Vigo, Spain
[6]Present address: Weill Cornell Medicine & New York Genome Center, New York, NY, USA
[7]Present address: Centro de Biomedicina Experimental (CEBEGA), Universidade de Santiago de Compostela, 15706 Santiago de Compostela, Spain
[8]Present address: Department of Pediatric Oncology, Dana-Farber Cancer Institute, Harvard, 21 Medical School, Boston, MA 02115, USA
[9]Present address: Institute of Solid State Electronics E362, Technische Universität Wien, Vienna, Austria
[10]These authors contributed equally
[11]Lead contact
*Correspondence: sonia.prado.gz@gmail.com (S.P.-L.), dposada@uvigo.es (D.P.)
https://doi.org/10.1016/j.crmeth.2025.101025

MOTIVATION Single-cell whole-genome amplification (scWGA) is a critical step for the genomic study of single cells, yet its impact on downstream analysis remains poorly understood. Previous studies were not comprehensive in the number of methods tested and the metrics assessed. Besides, they have mostly been conducted or replicated by the original authors of a method rather than by independent third-party laboratories. Here, we test six commercially available scWGA methods to understand their performance and propose a guide for selecting the best scWGA approach for studies on single-cell genomics.

SUMMARY

Single-cell genomics enables studying tissues and organisms at the highest resolution. However, since a cell contains a small amount of DNA, single-cell DNA sequencing (scDNA-seq) typically requires single-cell whole-genome amplification (scWGA). Unfortunately, scWGA methods introduce technical biases that complicate the interpretation of scDNA-seq data. We compared six scWGA methods, three MDA (multiple displacement amplification; GenomiPhi, REPLI-g, and TruePrime) and three non-MDA (Ampli1, MALBAC, and PicoPLEX), on 206 tumoral and 24 healthy human cells. scWGA methods performed differently depending on the parameter of interest. REPLI-g minimized regional amplification bias, while non-MDA methods showed a more uniform and reproducible amplification. Ampli1 exhibited the lowest allelic imbalance and dropout, the most accurate insertion or deletion (indel) and copy-number detection, and a low polymerase error rate. However, REPLI-g yielded higher DNA quantities, longer amplicons, and greater genome coverage. We offer a comprehensive guide for selecting a scWGA approach, outlining trade-offs that influence the interpretation of scDNA-seq data.

INTRODUCTION

Advances in single-cell genomics have made the study of genomic and transcriptomic variation possible at the most fundamental level, rapidly generating new insights into complex biological systems from microbial diversity to immune response, development, or tumor progression.[1–5] While single-cell RNA sequencing has been thoroughly developed, single-cell DNA sequencing (scDNA-seq) remains more elusive and challenging.[6–8] The difficulties of scDNA-seq mainly derive from the amplification step needed to sequence the small amount of DNA typically present in single cells (e.g., 6–7 pg in a human cell). Although whole-genome single-cell library preparation without preamplification is possible using direct tagmentation,[9–12] these strategies usually rely on microfluidic devices, which limits their adoption in standard research laboratories.

Most critically, tagmentation causes 50% random molecule loss, which prevents sensitive cell-level genotyping of variants other than copy numbers.[13] Finally, direct tagmentation methods necessitate the pooling and multiplexing of thousands of cells to generate sufficient library material, making them unsuitable for scenarios involving only one or a few cells. Therefore, single-cell whole-genome amplification (scWGA) is still a prerequisite in many applications of single-cell DNA genomics.

Multiple scWGA methods have been proposed, typically based on pure PCR,[14–17] multiple displacement amplification (MDA),[18–20] or a combination of both[21,22] but always relying on the use of DNA polymerases.[23] Unfortunately, DNA polymerases have a limited strand extension rate and processivity, and during scWGA, lots of priming and extension reactions are required.[24] This large amount of reactions entails significant technical errors such as (1) allelic imbalance, allelic dropout (ADO), and locus dropout (LDO), when a particular allele is preferentially amplified or not amplified at all or neither allele is amplified, respectively; (2) non-uniform coverage usually attributed to GC content affecting denaturation and primer binding efficiency[25–27]; (3) generation of chimeric DNA molecules originating false structural variants due to the polymerase strand displacement activity[28–30]; and (4) false single-nucleotide variants (SNVs) and insertions or deletions (indels) owing to the low fidelity of the DNA polymerase[26] (Figure S1A).

While several studies comparing the relative performance of different scWGA strategies have already been published, their scope is usually limited regarding the scWGA methods evaluated, the sequencing target, and the number and type of amplified cells[20,29–43] (Table S1). We are unaware of any study comparing many scWGA strategies on whole genomes obtained from many individual cells. Here, we report a comprehensive benchmark of six popular scWGA kits, over five next-generation sequencing (NGS) library preparation kits, and two NGS platforms using three human cell lines. In total, we obtained 230 single-cell whole-genome sequences under 54 experimental scenarios (Figure S1B). We show that MDA and non-MDA methods perform differently for distinct purposes and identify essential differences within these categories. Our results should help single-cell genomics researchers choose the best amplification method for their question of interest.

RESULTS

We assessed the performance of six scWGA commercial kits, three MDA (GenomiPhi, REPLI-g, and TruePrime) and three non-MDA (Ampli1, MALBAC, and PicoPLEX) (Figure S2; Table S2), and five library preparation kits (Table S3) in terms of amplification yield, amplicon size, genome breadth, amplification uniformity, allelic imbalance, ADO, LDO, erroneous bases, false SNVs, indels, copy numbers, and inversion and translocation breakpoints. To do this, we obtained low-pass (0.07–1.76×) whole-genome sequencing (WGS) data from 230 individual human cells from a healthy fibroblast cell line (HDF), a colorectal cancer cell line (Caco-2), and a mantle lymphoma cell line (Z-138). For the HDF cells, we completed a second WGS run at a higher depth (7.6–16.8×).

DNA yield and amplicon size

The amount of DNA obtained with the different scWGA kits and the size of the amplicons could be a limitation for downstream experiments. Here, we observed statistically significant differences among the scWGA methods in DNA yield and amplicon size, independently of the cell line (Figure 1; Table S4). REPLI-g provided the highest DNA yield by far, with a mean value across cell lines close to 35 μg, while the other scWGA kits produced average yields below 8 μg. For comparison, the average DNA yield from unamplified material (bulk; ∼1 million cells) was below 10 μg. MDA approaches (GenomiPhi, REPLI-g, and TruePrime) produced much larger amplicon sizes than non-MDA methods (Ampli1, MALBAC, and PicoPLEX) (around 10 and 1.2 kb on average, respectively). REPLI-g showed the largest amplicons (>30 kb), close to the average genomic DNA size obtained for the bulk (Figure 1B; Table S4). For both DNA yield and amplicon size, MDA methods were much more variable than non-MDA approaches, particularly in the case of REPLI-g, which displayed large standard deviations (Table S4).

Mapping rates and duplicated reads

For all scWGA methods, we observed a high percentage of mapped reads (Table S4), with marginally significant differences among them (p = 0.04). However, TruePrime showed many reads mapped to the mitochondrial genome (∼9% in Caco-2, ∼6% in Z-138, and ∼85% in HDF). Also, we identified clear mapping differences among the sequencing library kits ($p < 2.2e{-}16$; data not shown). Within these, the library protocols that include an enrichment PCR step (SureSelect and Nextera) showed a significantly higher percentage of mapped reads ($p = 3.8e{-}15$). Additionally, Ion Torrent produced significantly more duplicates than Illumina (averages of ∼25% and ∼5%, respectively; Figure S3A).

Genome breadth and amplification uniformity

An ideal scWGA method should provide a set of DNA molecules that represent the target genome as completely as possible. If the amplification is not uniform, then multiple genomic regions may be missed. We observed statistically significant differences among scWGA methods for amplification disuniformity (in comparison to the bulk; see STAR Methods) and genome breadth (i.e., the fraction of the genome covered by one or more reads) for the different cell lines. Thus, for 218 cells at 0.15× (we excluded 12 cells with lower depth from further analyses), Ampli1, MALBAC, and REPLI-g yielded the most extensive average genome breadth (8.5%–8.9%) close to the breadth observed for the bulk (12.1%), and TruePrime the lowest (4.1%), for all cell lines (Figure 2A; Table S4). For the higher-depth HDF dataset (24 cells downsampled at 7.6×), the results were qualitatively similar, with genome breadths of 64%, 58%, and 92% for REPLI-g, Ampli1, and bulk, respectively (Figure 2B). Again, TruePrime showed the lowest breadth (3%). For the pseudo-bulks (i.e., reads pooled across cells amplified with the same scWGA kit), MDA approaches showed the highest breadth (∼88%), with the exception of TruePrime (12%), while non-MDA strategies showed a genome breadth of around 70% (Figure 2B). On the other hand, at 0.15×, the amplifications were more uniform and reproducible for non-MDA methods than for

CellPress
OPEN ACCESS

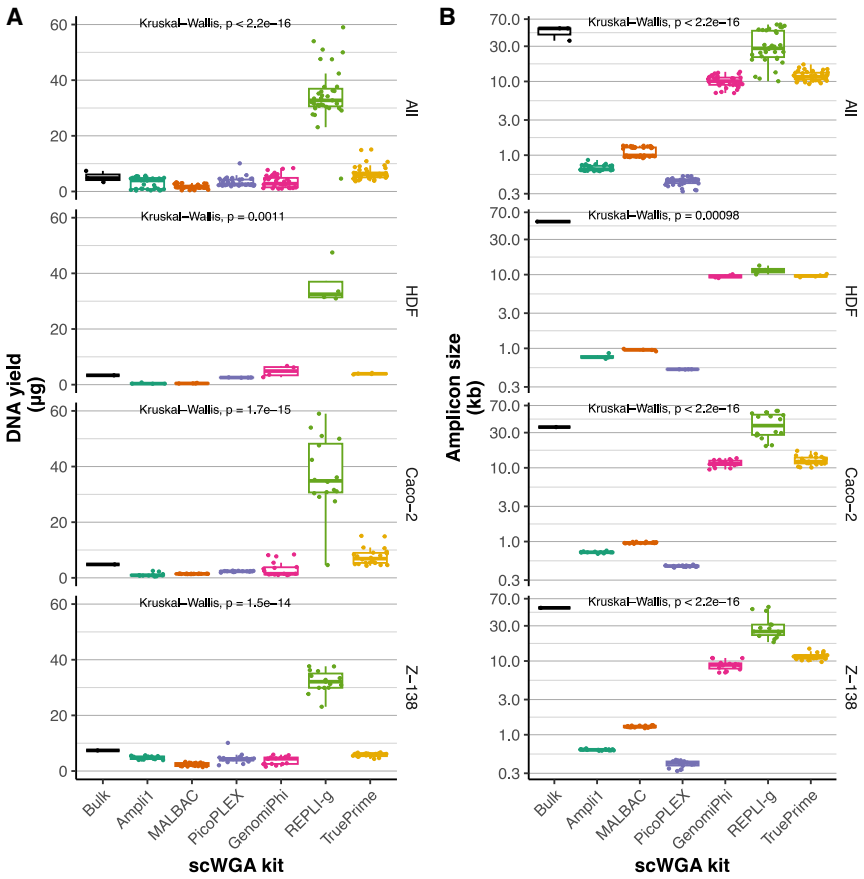

Figure 1. Amplification yield and amplicon size

Values are shown for all the cells together ("all") and for each cell line. Kruskal-Wallis test *p* values comparing all scWGA methods are indicated inside the plot. Results from the unamplified bulk ("bulk") are shown in the first column of each graph.

(A) DNA yield.

(B) Amplicon size (genomic DNA size for the bulk). Results are also shown by combining the three cell lines (all).

(A and B) Boxplots: the central line indicates the median, while the box limits correspond to the Q1 and Q3 quartiles; upper and lower whiskers extend from Q3 to Q3 + 1.5× (Q3 – Q1) and from Q1 to Q1 – 1.5× (Q3 – Q1), respectively.

See also Table S4.

MDA methods, with TruePrime performing the worst (Figures 2C and 2D; Table S4).

Albeit less dramatic, the library protocol also significantly affected genome breadth. For the combined cell lines, our modified KAPA protocol provided slightly more genome breadth at 0.15× than the other library protocols, with Nextera being the worst (Figure S3B). On the other hand, Nextera, SureSelect, and KAPA yielded slightly more uniform amplifications, although these differences were only marginally significant for Caco-2 (Figure S3C). The two sequencing technologies used, Illumina and Ion Torrent, did not significantly affect the amplification uniformity (Figure S3D).

Amplification recurrence

The coverage distribution along the genome observed for the HDF cells was significantly correlated with the coverage distribution of the unamplified bulk (Figure 3). Importantly, we found that two cells amplified with the same scWGA kit showed significantly more regions amplified in common than two cells amplified with a different scWGA kit, except for REPLI-g, which showed the same amplification recurrence with itself as with MALBAC (Figures 3 and S4A). In addition, we observed that non-MDA methods showed significantly higher coverage in regions with high GC content, as previously reported.[44] Interestingly, REPLI-g showed a negative coverage correlation with GC content, whereas the other MDA methods showed no preference based on sequence content.

Allelic imbalance, ADO, and LDO

During scWGA, a biased amplification of the two original alleles can cause a deviation of the expected allele frequencies at heterozygous sites (i.e., allelic imbalance) and even incorrect/missing genotype calls (ADO/LDO; Figure S4B). PicoPLEX and particularly Ampli1 outperformed the other methods regarding allelic imbalance and ADO rates (Figures 4A and 4B). Still, average ADO rates were significant, ranging from ∼16% for Ampli1 to ∼98% for TruePrime (Table S5). The observed LDO rates were highly correlated with the observed genome breadth values (Figure S4C). Here, the mean LDO values ranged from ∼36% for Ampli1 to ∼96% for TruePrime (Figure 4C; Table S5).

Erroneous bases, false SNVs, and indels

In the amplification process, the DNA polymerase can introduce erroneous bases (detected as alternative alleles, sometimes leading to false SNV calls) or insert/miss nucleotides into/from the template (which can lead to false indel calls). The proportions of erroneous bases at genomic positions in the single cells identified as homozygous in the HDF bulk were ∼0.3% for PicoPLEX and MALBAC and <0.1% for the other methods (TruePrime was the lowest) (Figure 5A; Table S5). These erroneous bases contribute to differences in false SNV rates, where Ampli1 (4.19e−5) and MDA methods (3.52e−5 to 6.83e−4) were between one and two orders of magnitude more accurate than MALBAC and PicoPLEX (Figure 5B; Table S5). False SNVs were biased toward transitions (Figure S4D). In terms of indel detection, sensitivity was highest for Ampli1 (87.7%) and lowest for TruePrime (63.9%), while PicoPLEX and MALBAC showed the lowest specificity (Figures 5C and 5D; Table S5).

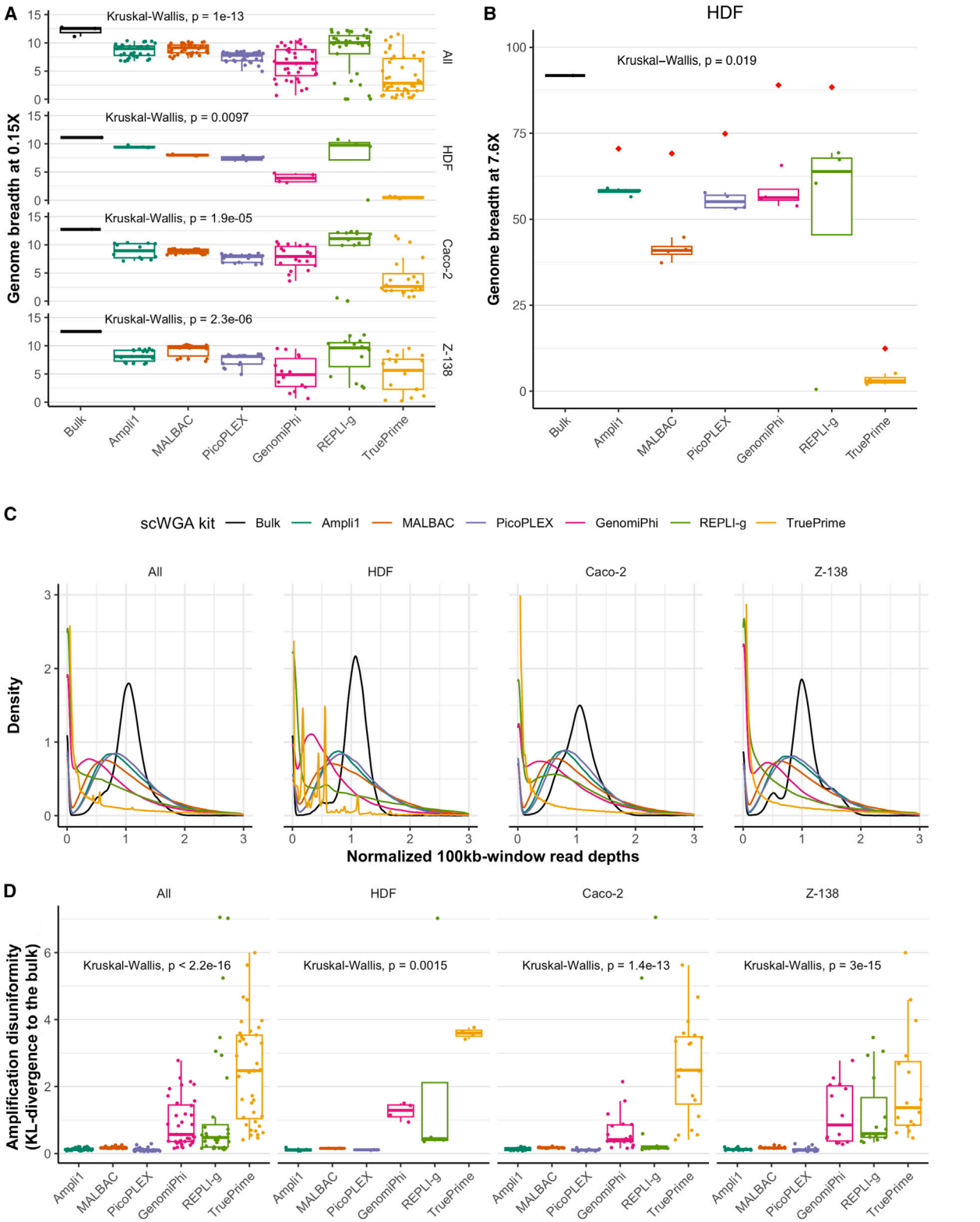

(legend on next page)

CellPress
OPEN ACCESS

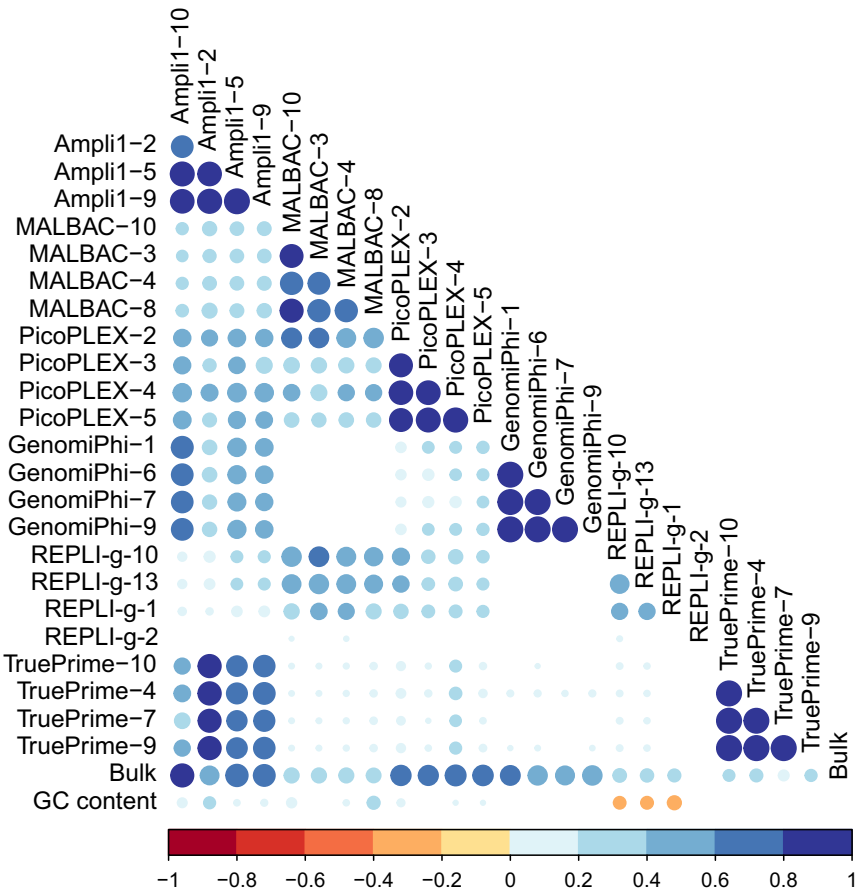

Figure 3. Amplification recurrence

Correlation of read counts between cells along 1-Mb-long genome windows for the HDF cell line at 7.6×. The size of the dots indicates the Pearson correlation coefficient value from low (small) to high (big), and they are colored differently if positive (blue scale) or negative (red scale). Only statistically significant values ($p < 0.05$) are shown. See also Figure S4A.

False structural variants

Copy-number aberrations, inversions, and translocations are structural variations of interest in assessing the genomic heterogeneity among cells. The copy-number variation (CNV) profiles were noisier for the MDA methods (Figure S5A). Accordingly, the coverage dispersion measure (MAD [median absolute deviation]),[45] which gives an indirect idea of the copy-number resolution, was, in general, significantly lower for non-MDA methods (Figure S5B). Although some of the TruePrime single cells achieved very low MAD values, this was likely due to cases with an excess of windows lacking actual coverage. The copy-number distances to the unamplified bulk increased overall with the segmentation bin size, except for TruePrime and some MALBAC and REPLI-g cells. Ampli1 provided the CNV profiles closest to the bulk, independently of the segmentation window size (Figure 6A). The segmentation is very dependent on the estimated ploidy value, which can, therefore, influence the accuracy of the CNV profiles (Figure S5C). CNV sensitivity and specificity depended on the size of the segmentation window (Figure S5D). On average, non-MDA methods were the most sensitive (>75%), although MALBAC's sensitivity comes at the expense of lower specificity (∼54%) (Figure S5E). On the other hand, MDA strategies were less sensitive and showed much more variance. In terms of specificity, Ampli1 was superior (∼91%), followed by PicoPLEX (∼80%) and GenomiPhi (∼74%). The CNV false positives were not biased toward gains or losses, although TruePrime often resulted in more false gains than false losses, while Ampli1 tended to show the opposite pattern (Figure S5F). Regarding the detection of structural variant breakpoints, REPLI-g showed the highest sensitivity and TruePrime the lowest (Figure 6B). However, these differences were non-statistically significant and likely resulted from a low number of true events, leading to very low counts of true positives and false negatives (Figures S6A and S6B). On the other hand, the differences in specificity were significant (p = 4.3e−3), with the non-MDA methods and, to a lesser extent, REPLI-g performing the best (Figure 6C). This result was due to the higher frequency of false positives in GenomiPhi and TruePrime; in this case, Ampli1 introduced the smallest number of false positives (Figure S6C).

DISCUSSION

In our experiments, MDA approaches (GenomiPhi, REPLI-g, and TruePrime) produced higher yields than non-MDA methods

Figure 2. Genome breadth and amplification disuniformity

(A, B, and D) Boxplots as in Figure 1.

(A and B) Effect of the scWGA method on genome breadth, measured by the percentage of the genome covered at 0.15× for all cell lines and at 7.6× for HDF. Results from the HDF pseudobulks (reads pooled across cells amplified with the same scWGA kit) at 7.6× are shown as red diamonds for each method. Breadth for the unamplified bulks is shown in the first column of each graph.

(C) Densities of the normalized read counts along genome windows spanning 100 kb constructed from the 0.15× data.

(D) Amplification disuniformity is measured as the Kullback-Leibler (K-L) divergence between the per-100 kb window read counts of each single cell and the bulk. The higher the K-L divergence to the bulk, the higher the amplification disuniformity.

See also Figure S3 and Table S4.

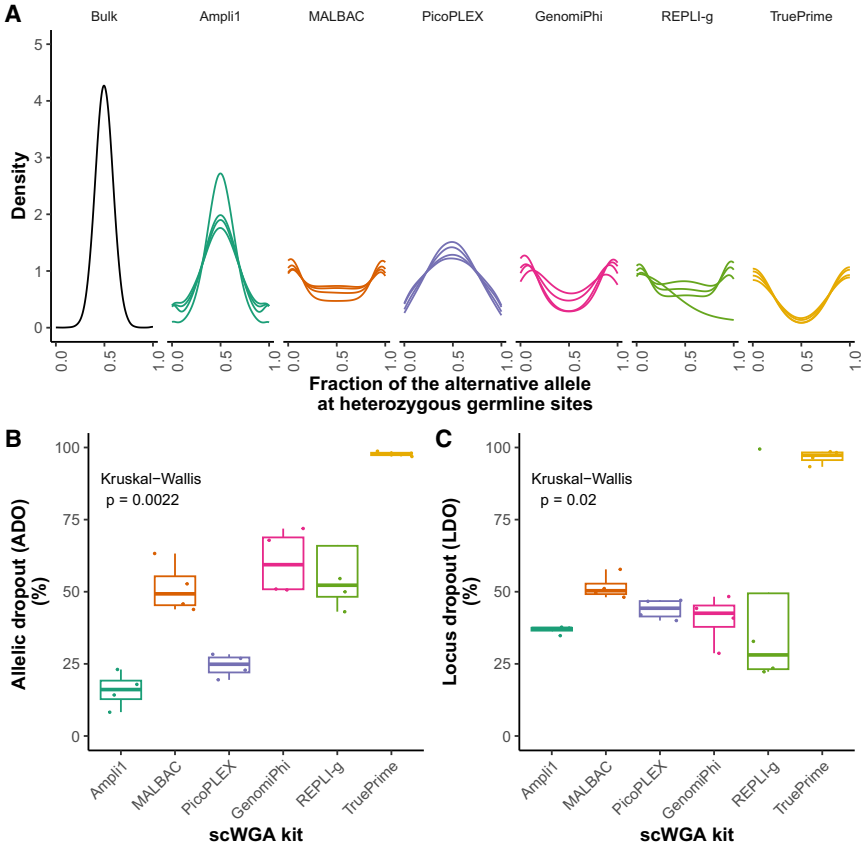

Figure 4. Allelic imbalance, ADO, and LDO for the HDF cell line

(A) Kernel density estimation of the alternative allele fraction at heterozygous germline sites. Each line within a panel tab represents a different cell. Each cell was sequenced at an average depth of 7.6×. Here, we used 100,000 heterozygous positions with at least 15 reads of coverage in the HDF bulk.

(B) ADO.

(C) LDO.

(B and C) Measurements were carried out along chromosome 1. Boxplots are as in Figure 1.

See also Figures S4B and S4C and Table S5.

(Ampli1, MALBAC, and PicoPLEX), which could be related to a more stable polymerase activity under isothermal conditions.[46] At the same time, MDA approaches generated larger amplicon sizes than non-MDA methods, likely due to a higher processing capability and template affinity of the Phi29 DNA polymerase.[47–49] In particular, REPLI-g outperformed the other scWGA strategies in this aspect, possibly resulting from a higher DNA polymerase concentration.[50]

Not surprisingly, the amplification protocols only marginally affected the mapping rates. While the scWGA kit employed had a much smaller effect on the percentage of mapped reads than the library construction method—strategies with an enrichment PCR step like SureSelect and Nextera were better—in all cases, these percentages were relatively high (data not shown). Ion Torrent sequencing resulted in significantly more duplicates than Illumina, probably due to the emulsion PCR step included in its protocol.[51]

REPLI-g resulted in the highest breadth, as previously reported,[29,30,34,43,52] which can likely be explained by its ability to initiate long amplicons at almost any genomic location. As expected, Ampli1 showed more breadth than the other two non-MDA methods.[43] Similarly, this trend was also observed in the pseudobulks (i.e., pooled reads across cells amplified with the same method), with MDA methods resulting in higher breadths than non-MDA methods, excluding TruePrime. Non-MDA methods amplified the genome more uniformly than MDA approaches, consistent with previous findings.[30,32–34,42] We attribute this result to the controlled PCR process based on exponential amplification cycles, which are absent in the isothermal acyclic MDA reactions. TruePrime produced the least uniform amplifications, which aligns with its lowest genome breadth. The lysis and denaturation steps of TruePrime take place on ice, which might prevent the availability of single-stranded DNA for the primase,[46] affecting breadth and amplification uniformity.

A correlation of the coverage along the genome between single cells and the unamplified bulk was anticipated, mainly due to mappability limitations for repetitive sequences.[53] However, unless there is a recurrent amplification bias, we would not expect to see a higher correlation among cells amplified with the same scWGA kit than cells amplified with a different scWGA kit or with the bulk. Therefore, our results suggest that the different scWGA kits tend to amplify the same regions, although the recurrence is lower for REPLI-g. We expect spatial recurrence in the amplification for non-MDA methods because they use their own non-random primers. For MDA methods, the results are more challenging to interpret. GenomiPhi and REPLI-g use random primers, while TruePrime's primase generates its primers, with the latter process being potentially less random.[19] Besides, the differences in the DNA denaturation conditions among the MDA kits might also affect spatial recurrence due to dissimilarities in DNA template availability.[46] Strikingly, none of the MDA approaches showed a random amplification pattern, although the recurrence was not as strong for REPLI-g. Zhang et al.[24] obtained a better fit with a statistical model with random amplification bias for MDA, but they did not clarify which MDA method they used.

For the HDF cell line, the non-MDA methods, except for MALBAC, showed a distribution for the alternative allele frequency in heterozygous germline sites more similar to the bulk, clearly outperforming the MDA methods in terms of allelic imbalance. In particular, Ampli1 produced a very low allelic imbalance. This sought behavior of Ampli1 might result from a synthesis

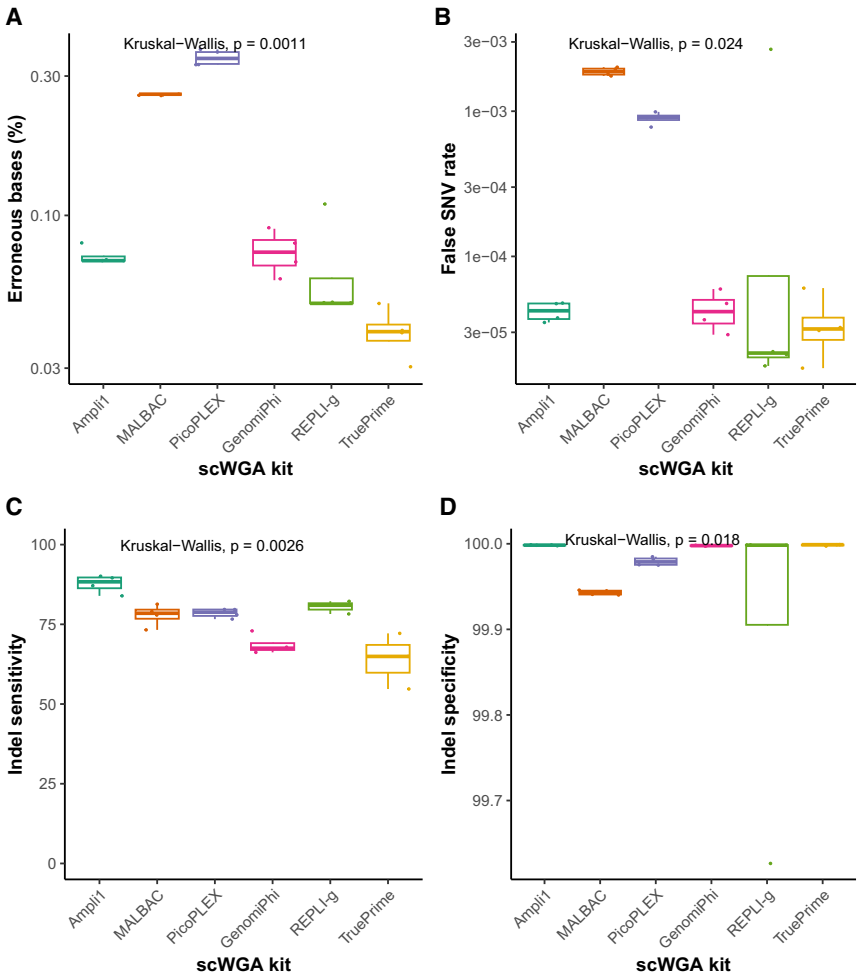

Figure 5. Erroneous bases, false SNV rate, and indel sensitivity and specificity for the HDF cell line

Boxplots are as in Figure 1.

(A) Percentage of alternative bases at sites genotyped as homozygous in the bulk.

(B) False SNV rate.

(C) Indel sensitivity.

(D) Indel specificity. Measurements were carried out on chromosome 1.

See Figure S4D and Table S5.

procedure that converts residual single-strand DNA (ssDNA) molecules into double-strand DNA (dsDNA) molecules. In agreement with these results—ADO is an extreme case of allelic imbalance—PicoPLEX and particularly Ampli1 showed lower ADO rates than the other methods. Conversely, TruePrime showed a substantial ADO rate (~98%). Still, the observed 16% average ADO rate for Ampli1 is slightly higher than previously reported.[37,54,55] Here, the estimated ADO rates for MDA methods were high (>60%), as observed by others.[37,40,56]

We found significant differences among methods regarding the proportion of erroneous bases, false SNVs, and false indels, suggesting different amplification error rates. The average false SNV rates, between 3.5e−5 and 1.9e−3, were generally in the range of previous estimates.[30,34,57,58] In principle, we expect MDA methods to show lower error rates due to the use of *Phi29*, a DNA polymerase with higher fidelity than those used by non-MDA methods.[23,26,49] In agreement with this idea, MALBAC showed the highest false SNV rate. Furthermore, a fraction of these apparent errors might be proper somatic variants, so the absolute value of the amplification error might be inflated to some extent. However, this bias should not be significant, as healthy fibroblasts should not possess extensive somatic variation. In any case, consensus/census approaches, where only mutations seen in more than one cell are trusted, or linked-read strategies should dramatically reduce this rate.[24,59–61] Interestingly, the different scWGA methods evaluated here showed distinct error profiles. However, they all showed an excess of C:G>T:A transitions, previously attributed to high-temperature denaturation protocols.[62] Being aware of different error signatures for some scWGA kits is a fact to consider if one is interested in single-cell mutational signatures. For indel detection, Ampli1 was superior, which might be related to the type of polymerase used and the level of ADO.[37,63]

According to Ginkgo, the HDF copy-number profiles were very accurate for Ampli1, no matter the segmentation window size. On the contrary, PicoPLEX and GenomiPhi seem to benefit from larger window sizes, whereas REPLI-g, MALBAC, and particularly TruePrime were less predictable. Although the read counts were generally more dispersed for the MDA methods, this apparent dispersion was not always directly related to the accuracy of the copy-number profiles. Regarding inversion and translocation breakpoints, the absolute number of false positives was noticeably different, with Ampli1 performing the best. The superiority of Ampli1 is expected, given that it does not use a polymerase with strand displacement activity, which can create spurious chimeric amplicons.[28,64,65]

This benchmark focuses on popular, reproducible, out-of-the-box methods for scWGA, which are likely to see widespread use. Other homemade protocols exist for scWGA, like LIANTI,[58] and other MDA modifications have also been proposed.[62,66] As far as we know, these methods have only been implemented by the authors who developed them, so they have yet to be extensively validated by third parties. When we carried out these experiments, primary template-directed amplification (PTA; now ResolveDNA[20]) was not commercialized, so we could not test it under the same conditions.

In conclusion, none of the scWGA methods tested here outperformed the others in all scenarios assessed, but some

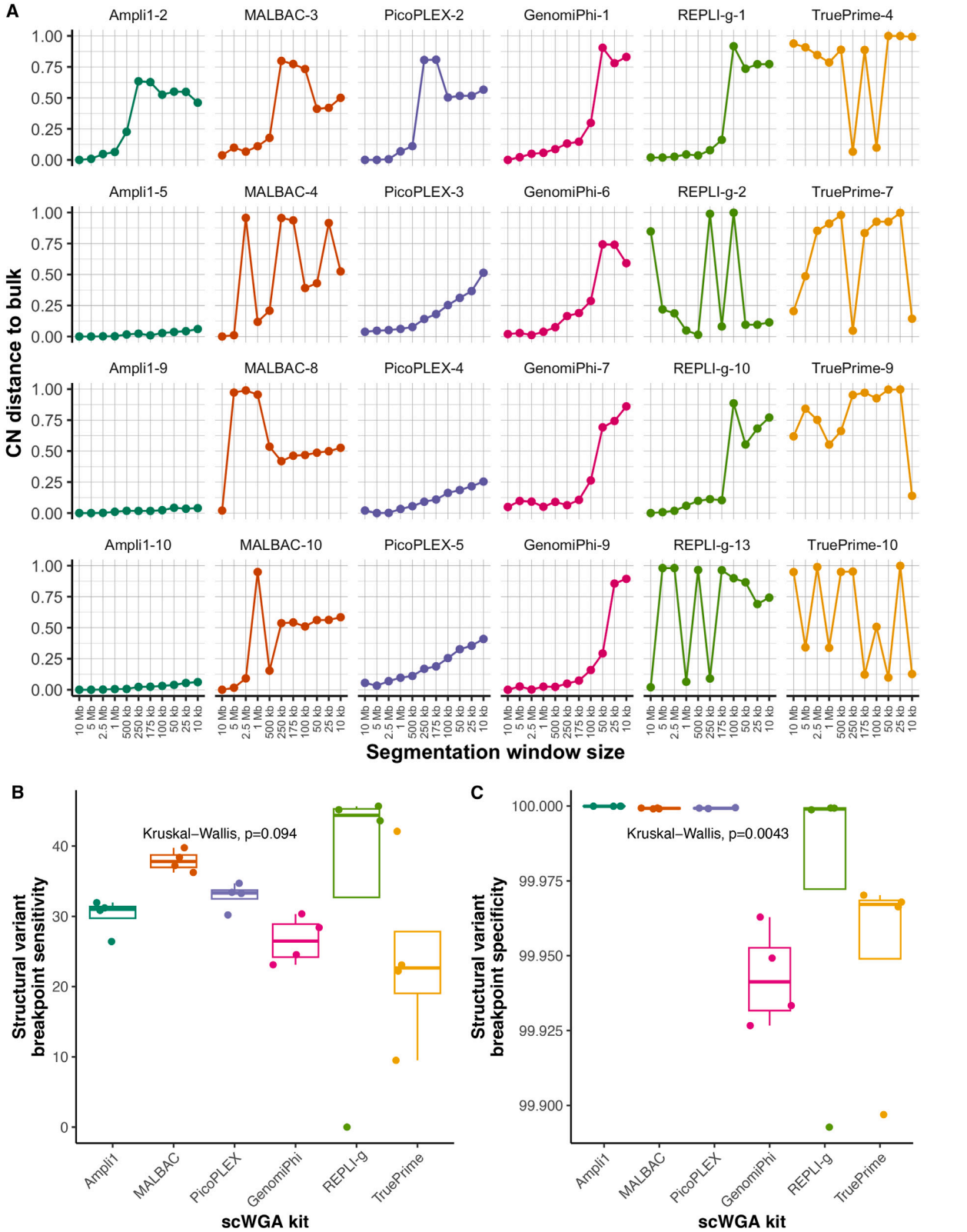

(legend on next page)

Table 1. Strengths and weaknesses of the six scWGA kits tested

scWGA kit	Ampli1	MALBAC	PicoPLEX	GenomiPhi	REPLI-g	TruePrime
Genome breadth	+	–	+	+	++	–
Amplification disuniformity	++	+	++	–	–	–
Amplification recurrence	++	+	++	++	–	++
ADO	++	–	+	–	–	–
False SNV rate	+	–	–	+	+	+
Indel calling	++	–	–	–	+	–
CNV calling	++	–	–	–	–	–
SV calling	++	++	++	–	+	–
Price per reaction (€)[a]	28.5	34	36	20	31.5	15

++, very good performance; +, good performance; –, inferior performance; ADO, allelic dropout; SNV, single-nucleotide variant; CNV, copy-number variant; SV, structural variant.
[a]Prices only include the scWGA reagents. The price is as of November 2024 for the currently available versions of the kits.

are better than others in different aspects (Table 1). For tracking cell lineages, which are key in cancer evolution or neurobiology, we should use a method that tends to amplify homologous regions. In this case, REPLI-g is not the best option. Ampli1 might be the method of choice for prenatal screening, given its copy-number profiles' accuracy and low ADO. In cancer genomics, where ploidy alterations can be significant, Ampli1 might also be the best option. For *de novo* unicellular genome assembly, a method like REPLI-g, with large amplicon sizes and not too many false structural variants, could be optimal. However, its lack of reproducibility might be somehow problematic.

Limitations of the study

Our amplification error estimations are inherently relative because it is not feasible to fully distinguish amplification errors from real healthy somatic variation in cell lines. Using genetically closer cells (i.e., kindred cells) could mitigate this issue. Increasing the number of cells in the study should help to obtain more accurate metrics and reduce the impact of outliers.

RESOURCE AVAILABILITY

Lead contact

All requests for reagents and resources should be directed to the lead contact, David Posada (dposada@uvigo.es).

Materials availability

This study did not generate new unique reagents.

Data and code availability

- Bulk and single-cell FASTQ files generated for this study have been deposited at the Sequence Read Archive under STUDY accession SRA: PRJNA494024.
- The scripts used for this study are available in the following repository: https://gitlab.com/phylocancer/scwga-benchmark/.
- Any additional information required to reanalyze the data reported in this study is available from the lead contact upon request.

ACKNOWLEDGMENTS

This work was supported by the European Research Council (ERC-617457-PHYLOCANCER awarded to D.P.) and by the Spanish Ministry of Science, Innovation, and Universities - MCIU (PID2019-106247GB-I00 awarded to D.P.). D.P. received further support from Xunta de Galicia. N.E.-G. was supported by a PhD fellowship from the Galician government (ED481A-2015/475). T.P. was supported by a PhD fellowship from the Spanish government (FPU15/03709) and, previously, by a PhD fellowship from the Galician government (ED481A-2015/083). L.T. was supported by a PhD fellowship from the Galician government (ED481A-2018/303). H.H. is a Miguel Servet (CP14/00229) researcher funded by the Spanish Institute of Health Carlos III (ISCIII). H.H. received funding from the Ministerio de Ciencia, Innovación y Universidades (SAF2017-89109-P; AEI/FEDER, UE). Core funding is from the ISCIII and the Generalitat de Catalunya. We want to thank Mercedes Peleteiro, the flow cytometry core facility manager, for her help and support; people from the Fundación Pública Galega de Medicina Xenómica (FPGMX) for their help with some of the experiments; and Joao Alves, Harald Detering, Fabián Crespo, Xose S. Puente, and Andrés Pérez-Figueroa for discussions. We thank the Supercomputation Center of Galicia (CESGA) for providing computational resources.

AUTHOR CONTRIBUTIONS

D.P. designed the project and supervised the whole study. N.E.-G., S.P.-L., P.A., A.G.-A., and H.H. performed the experiments. T.P. and L.T. carried out the bioinformatic analyses. N.E.-G. and T.P. performed the statistical analyses. N.E.-G., T.P., L.T., S.P.-L., and D.P. wrote the manuscript. All authors read, commented on, and approved the final manuscript.

DECLARATION OF INTERESTS

H.H. is a cofounder and shareholder of Omniscope, a scientific advisory board member of MiRXES and Nanostring, and a consultant to Moderna and Singularity.

Figure 6. False structural variants for the HDF cell line

(A) Distance of each single-cell CNV profile to the bulk measured as the percentage of bases erroneously assigned to a copy-number state times the total length of the profile.
(B and C) Sensitivity and specificity of structural variant breakpoints for the different scWGA kits. Boxplots are as in Figure 1.
See Figures S5 and S6.

STAR★METHODS

Detailed methods are provided in the online version of this paper and include the following:

- KEY RESOURCES TABLE
- EXPERIMENTAL MODEL AND STUDY PARTICIPANT DETAILS
  - Cell lines
- METHOD DETAILS
  - Single-cell isolation
  - Single-cell whole-genome amplification (scWGA)
  - Bulk DNA extraction
  - Next-generation sequencing libraries
  - Whole-genome sequencing
  - Preprocessing of NGS data
  - Mapping rates and duplicates
  - Genome breadth
  - Amplification disuniformity
  - Amplification recurrence
  - Allelic imbalance, ADO, and LDO
  - Amplification polymerase errors
  - Copy number
  - Structural variant breakpoints
- QUANTIFICATION AND STATISTICAL ANALYSIS

SUPPLEMENTAL INFORMATION

Supplemental information can be found online at https://doi.org/10.1016/j.crmeth.2025.101025.

Received: June 12, 2024
Revised: December 5, 2024
Accepted: March 20, 2025
Published: April 21, 2025

REFERENCES

1. Kaster, A.-K., and Sobol, M.S. (2020). Microbial single-cell omics: the crux of the matter. Appl. Microbiol. Biotechnol. *104*, 8209–8220. https://doi.org/10.1007/s00253-020-10844-0.
2. Pfisterer, U., Bräunig, J., Brattås, P., Heidenblad, M., Karlsson, G., and Fioretos, T. (2021). Single-cell sequencing in translational cancer research and challenges to meet clinical diagnostic needs. Genes Chromosomes Cancer *60*, 504–524. https://doi.org/10.1002/gcc.22944.
3. Evrony, G.D., Hinch, A.G., and Luo, C. (2021). Applications of Single-Cell DNA Sequencing. Annu. Rev. Genomics Hum. Genet. *22*, 171–197. https://doi.org/10.1146/annurev-genom-111320-090436.
4. Kojima, M., Harada, T., Fukazawa, T., Kurihara, S., Touge, R., Saeki, I., Takahashi, S., and Hiyama, E. (2023). Single-cell next-generation sequencing of circulating tumor cells in patients with neuroblastoma. Cancer Sci. *114*, 1616–1624. https://doi.org/10.1111/cas.15707.
5. Qu, S., Gong, M., Deng, Y., Xiang, Y., and Ye, D. (2024). Research progress and application of single-cell sequencing in head and neck malignant tumors. Cancer Gene Ther. *31*, 18–27. https://doi.org/10.1038/s41417-023-00691-2.
6. Linnarsson, S., and Teichmann, S.A. (2016). Single-cell genomics: coming of age. Genome Biol. *17*, 97. https://doi.org/10.1186/s13059-016-0960-x.
7. Lähnemann, D., Köster, J., Fischer, U., Borkhardt, A., McHardy, A.C., and Schönhuth, A. (2021). Accurate and scalable variant calling from single cell DNA sequencing data with ProSolo. Nat. Commun. *12*, 6744. https://doi.org/10.1038/s41467-021-26938-w.
8. Melnekoff, D.T., and Laganà, A. (2022). Single-Cell Sequencing Technologies in Precision Oncology. Comput. Methods Precis. Oncol. *1361*, 269–282. https://doi.org/10.1007/978-3-030-91836-1_15.
9. Zahn, H., Steif, A., Laks, E., Eirew, P., VanInsberghe, M., Shah, S.P., Aparicio, S., and Hansen, C.L. (2017). Scalable whole-genome single-cell library preparation without preamplification. Nat. Methods *14*, 167–173. https://doi.org/10.1038/nmeth.4140.
10. Xi, L., Belyaev, A., Spurgeon, S., Wang, X., Gong, H., Aboukhalil, R., and Fekete, R. (2017). New library construction method for single-cell genomes. PLoS One *12*, e0181163. https://doi.org/10.1371/journal.pone.0181163.
11. Laks, E., McPherson, A., Zahn, H., Lai, D., Steif, A., Brimhall, J., Biele, J., Wang, B., Masud, T., Ting, J., et al. (2019). Clonal Decomposition and DNA Replication States Defined by Scaled Single-Cell Genome Sequencing. Cell *179*, 1207–1221.e22. https://doi.org/10.1016/j.cell.2019.10.026.
12. Minussi, D.C., Nicholson, M.D., Ye, H., Davis, A., Wang, K., Baker, T., Tarabichi, M., Sei, E., Du, H., Rabbani, M., et al. (2021). Breast Tumors Maintain a Reservoir of Subclonal Diversity During Expansion. Nature *592*, 302–308. https://doi.org/10.1038/s41586-021-03357-x.
13. Adey, A.C. (2021). Tagmentation-based single-cell genomics. Genome Res. *31*, 1693–1705. https://doi.org/10.1101/gr.275223.121.
14. Nelson, D.L., Ledbetter, S.A., Corbo, L., Victoria, M.F., Ramírez-Solis, R., Webster, T.D., Ledbetter, D.H., and Caskey, C.T. (1989). Alu polymerase chain reaction: a method for rapid isolation of human-specific sequences from complex DNA sources. Proc. Natl. Acad. Sci. USA *86*, 6686–6690.
15. Zhang, L., Cui, X., Schmitt, K., Hubert, R., Navidi, W., and Arnheim, N. (1992). Whole genome amplification from a single cell: implications for genetic analysis. Proc. Natl. Acad. Sci. USA *89*, 5847–5851.
16. Telenius, H., Carter, N.P., Bebb, C.E., Nordenskjöld, M., Ponder, B.A., and Tunnacliffe, A. (1992). Degenerate oligonucleotide-primed PCR: general amplification of target DNA by a single degenerate primer. Genomics *13*, 718–725.
17. Klein, C.A., Schmidt-Kittler, O., Schardt, J.A., Pantel, K., Speicher, M.R., and Riethmüller, G. (1999). Comparative genomic hybridization, loss of heterozygosity, and DNA sequence analysis of single cells. Proc. Natl. Acad. Sci. USA *96*, 4494–4499. https://doi.org/10.1073/pnas.96.8.4494.
18. Dean, F.B., Hosono, S., Fang, L., Wu, X., Faruqi, A.F., Bray-Ward, P., Sun, Z., Zong, Q., Du, Y., Du, J., et al. (2002). Comprehensive human genome amplification using multiple displacement amplification. Proc. Natl. Acad. Sci. USA *99*, 5261–5266. https://doi.org/10.1073/pnas.082089499.
19. Picher, Á.J., Budeus, B., Wafzig, O., Krüger, C., García-Gómez, S., Martínez-Jiménez, M.I., Díaz-Talavera, A., Weber, D., Blanco, L., and Schneider, A. (2016). TruePrime is a novel method for whole-genome amplification from single cells based on TthPrimPol. Nat. Commun. *7*, 13296. https://doi.org/10.1038/ncomms13296.
20. González-Pena, V., Natarajan, S., Xia, Y., Klein, D., Carter, R., Pang, Y., Shaner, B., Annu, K., Putnam, D., Chen, W., et al. (2021). Accurate genomic variant detection in single cells with primary template-directed amplification. Proc. Natl. Acad. Sci. USA *118*, e2024176118. https://doi.org/10.1073/pnas.2024176118.
21. Kamberov, E., Sun, T., Bruening, E., Pinter, J.H., Sleptsova, I., Kurihara, T., and Makarov, V.L. (2012). Amplification and analysis of whole genome and whole transcriptome libraries generated by a DNA polymerization process. US patent. filed March 3, 2010, and published June 26, 2012.
22. Zong, C., Lu, S., Chapman, A.R., and Xie, X.S. (2012). Genome-wide detection of single-nucleotide and copy-number variations of a single human cell. Science *338*, 1622–1626. https://doi.org/10.1126/science.1229164.
23. Ordóñez, C.D., and Redrejo-Rodríguez, M. (2023). DNA Polymerases for Whole Genome Amplification: Considerations and Future Directions. Int. J. Mol. Sci. *24*, 9331. https://doi.org/10.3390/ijms24119331.
24. Zhang, C.-Z., Adalsteinsson, V.A., Francis, J., Cornils, H., Jung, J., Maire, C., Ligon, K.L., Meyerson, M., and Love, J.C. (2015). Calibrating genomic and allelic coverage bias in single-cell sequencing. Nat. Commun. *6*, 6822. https://doi.org/10.1038/ncomms7822.

25. Hou, Y., Song, L., Zhu, P., Zhang, B., Tao, Y., Xu, X., Li, F., Wu, K., Liang, J., Shao, D., et al. (2012). Single-cell exome sequencing and monoclonal evolution of a JAK2-negative myeloproliferative neoplasm. Cell *148*, 873–885. https://doi.org/10.1016/j.cell.2012.02.028.

26. Navin, N.E. (2014). Cancer genomics: one cell at a time. Genome Biol. *15*, 452. https://doi.org/10.1186/s13059-014-0452-9.

27. Sabina, J., and Leamon, J.H. (2015). Bias in Whole Genome Amplification: Causes and Considerations. Methods Mol. Biol. *1347*, 15–41. https://doi.org/10.1007/978-1-4939-2990-0_2.

28. Lasken, R.S., and Stockwell, T.B. (2007). Mechanism of chimera formation during the Multiple Displacement Amplification reaction. BMC Biotechnol. *7*, 19. https://doi.org/10.1186/1472-6750-7-19.

29. Voet, T., Kumar, P., Van Loo, P., Cooke, S.L., Marshall, J., Lin, M.-L., Zamani Esteki, M., Van der Aa, N., Mateiu, L., McBride, D.J., et al. (2013). Single-cell paired-end genome sequencing reveals structural variation per cell cycle. Nucleic Acids Res. *41*, 6119–6138. https://doi.org/10.1093/nar/gkt345.

30. Huang, L., Ma, F., Chapman, A., Lu, S., and Xie, X.S. (2015). Single-Cell Whole-Genome Amplification and Sequencing: Methodology and Applications. Annu. Rev. Genomics Hum. Genet. *16*, 79–102. https://doi.org/10.1146/annurev-genom-090413-025352.

31. Chen, M., Song, P., Zou, D., Hu, X., Zhao, S., Gao, S., and Ling, F. (2014). Comparison of multiple displacement amplification (MDA) and multiple annealing and looping-based amplification cycles (MALBAC) in single-cell sequencing. PLoS One *9*, e114520. https://doi.org/10.1371/journal.pone.0114520.

32. de Bourcy, C.F.A., De Vlaminck, I., Kanbar, J.N., Wang, J., Gawad, C., and Quake, S.R. (2014). A Quantitative Comparison of Single-Cell Whole Genome Amplification Methods. PLoS One *9*, e105585. https://doi.org/10.1371/journal.pone.0105585.

33. Ning, L., Li, Z., Wang, G., Hu, W., Hou, Q., Tong, Y., Zhang, M., Chen, Y., Qin, L., Chen, X., et al. (2015). Quantitative assessment of single-cell whole genome amplification methods for detecting copy number variation using hippocampal neurons. Sci. Rep. *5*, 11415. https://doi.org/10.1038/srep11415.

34. Hou, Y., Wu, K., Shi, X., Li, F., Song, L., Wu, H., Dean, M., Li, G., Tsang, S., Jiang, R., et al. (2015). Comparison of variations detection between whole-genome amplification methods used in single-cell resequencing. GigaScience *4*, 37. https://doi.org/10.1186/s13742-015-0068-3.

35. Deleye, L., De Coninck, D., Christodoulou, C., Sante, T., Dheedene, A., Heindryckx, B., Van den Abbeel, E., De Sutter, P., Menten, B., Deforce, D., and Van Nieuwerburgh, F. (2015). Whole genome amplification with SurePlex results in better copy number alteration detection using sequencing data compared to the MALBAC method. Sci. Rep. *5*, 11711. https://doi.org/10.1038/srep11711.

36. Li, N., Wang, L., Wang, H., Ma, M., Wang, X., Li, Y., Zhang, W., Zhang, J., Cram, D.S., and Yao, Y. (2015). The Performance of Whole Genome Amplification Methods and Next-Generation Sequencing for Pre-Implantation Genetic Diagnosis of Chromosomal Abnormalities. J. Genet. Genomics *42*, 151–159. https://doi.org/10.1016/j.jgg.2015.03.001.

37. Babayan, A., Alawi, M., Gormley, M., Müller, V., Wikman, H., McMullin, R.P., Smirnov, D.A., Li, W., Geffken, M., Pantel, K., and Joosse, S.A. (2017). Comparative study of whole genome amplification and next generation sequencing performance of single cancer cells. Oncotarget *8*, 56066–56080. https://doi.org/10.18632/oncotarget.10701.

38. Deleye, L., De Coninck, D., Dheedene, A., De Sutter, P., Menten, B., Deforce, D., and Van Nieuwerburgh, F. (2016). Performance of a TthPrimPol-based whole genome amplification kit for copy number alteration detection using massively parallel sequencing. Sci. Rep. *6*, 31825. https://doi.org/10.1038/srep31825.

39. Deleye, L., Tilleman, L., Vander Plaetsen, A.-S., Cornelis, S., Deforce, D., and Van Nieuwerburgh, F. (2017). Performance of four modern whole genome amplification methods for copy number variant detection in single cells. Sci. Rep. *7*, 3422. https://doi.org/10.1038/s41598-017-03711-y.

40. Borgström, E., Paterlini, M., Mold, J.E., Frisen, J., and Lundeberg, J. (2017). Comparison of whole genome amplification techniques for human single cell exome sequencing. PLoS One *12*, e0171566. https://doi.org/10.1371/journal.pone.0171566.

41. Deleye, L., Gansemans, Y., De Coninck, D., Van Nieuwerburgh, F., and Deforce, D. (2018). Massively parallel sequencing of micro-manipulated cells targeting a comprehensive panel of disease-causing genes: A comparative evaluation of upstream whole-genome amplification methods. PLoS One *13*, e0196334.

42. Lu, S., Chang, C.-J., Guan, Y., Szafer-Glusman, E., Punnoose, E., Do, A., Suttmann, B., Gagnon, R., Rodriguez, A., Landers, M., et al. (2020). Genomic Analysis of Circulating Tumor Cells at the Single-Cell Level. J. Mol. Diagn. *22*, 770–781. https://doi.org/10.1016/j.jmoldx.2020.02.013.

43. Biezuner, T., Raz, O., Amir, S., Milo, L., Adar, R., Fried, Y., Ainbinder, E., and Shapiro, E. (2021). Comparison of seven single cell Whole Genome Amplification commercial kits using targeted sequencing. Sci. Rep. *11*, 17171. https://doi.org/10.1038/s41598-021-96045-9.

44. Benjamini, Y., and Speed, T.P. (2012). Summarizing and correcting the GC content bias in high-throughput sequencing. Nucleic Acids Res. *40*, e72. https://doi.org/10.1093/nar/gks001.

45. Garvin, T., Aboukhalil, R., Kendall, J., Baslan, T., Atwal, G.S., Hicks, J., Wigler, M., and Schatz, M.C. (2015). Interactive analysis and assessment of single-cell copy-number variations. Nat. Methods *12*, 1058–1060. https://doi.org/10.1038/nmeth.3578.

46. Pinard, R., de Winter, A., Sarkis, G.J., Gerstein, M.B., Tartaro, K.R., Plant, R.N., Egholm, M., Rothberg, J.M., and Leamon, J.H. (2006). Assessment of whole genome amplification-induced bias through high-throughput, massively parallel whole genome sequencing. BMC Genom. *7*, 216. https://doi.org/10.1186/1471-2164-7-216.

47. Blanco, L., Bernad, A., Lázaro, J.M., Martín, G., Garmendia, C., and Salas, M. (1989). Highly efficient DNA synthesis by the phage phi 29 DNA polymerase. Symmetrical mode of DNA replication. J. Biol. Chem. *264*, 8935–8940.

48. de Paz, A.M., Cybulski, T.R., Marblestone, A.H., Zamft, B.M., Church, G.M., Boyden, E.S., Kording, K.P., and Tyo, K.E.J. (2018). High-resolution mapping of DNA polymerase fidelity using nucleotide imbalances and next-generation sequencing. Nucleic Acids Res. *46*, e78. https://doi.org/10.1093/nar/gky296.

49. Wang, X., Liu, Y., Liu, H., Pan, W., Ren, J., Zheng, X., Tan, Y., Chen, Z., Deng, Y., He, N., et al. (2022). Recent advances and application of whole genome amplification in molecular diagnosis and medicine. MedComm *3*, e116. https://doi.org/10.1002/mco2.116.

50. Dimitriadou, E., Zamani Esteki, M., and Vermeesch, J.R. (2015). Copy Number Variation Analysis by Array Analysis of Single Cells Following Whole Genome Amplification. Methods Mol. Biol. *1347*, 197–219. https://doi.org/10.1007/978-1-4939-2990-0_14.

51. Balzer, S., Malde, K., Grohme, M.A., and Jonassen, I. (2013). Filtering duplicate reads from 454 pyrosequencing data. Bioinformatics *29*, 830–836. https://doi.org/10.1093/bioinformatics/btt047.

52. Chen, D., Zhen, H., Qiu, Y., Liu, P., Zeng, P., Xia, J., Shi, Q., Xie, L., Zhu, Z., Gao, Y., et al. (2018). Comparison of single cell sequencing data between two whole genome amplification methods on two sequencing platforms. Sci. Rep. *8*, 4963. https://doi.org/10.1038/s41598-018-23325-2.

53. Treangen, T.J., and Salzberg, S.L. (2011). Repetitive DNA and next-generation sequencing: computational challenges and solutions. Nat. Rev. Genet. *13*, 36–46. https://doi.org/10.1038/nrg3117.

54. Binder, V., Bartenhagen, C., Okpanyi, V., Gombert, M., Moehlendick, B., Behrens, B., Klein, H.-U., Rieder, H., Ida Krell, P.F., Dugas, M., et al. (2014). A New Workflow for Whole-Genome Sequencing of Single Human Cells. Hum. Mutat. *35*, 1260–1270.

55. Normand, E., Qdaisat, S., Bi, W., Shaw, C., Van den Veyver, I., Beaudet, A., and Breman, A. (2016). Comparison of three whole genome

amplification methods for detection of genomic aberrations in single cells. Prenat. Diagn. *36*, 823–830. https://doi.org/10.1002/pd.4866.

56. Leung, M.L., Wang, Y., Waters, J., and Navin, N.E. (2015). SNES: single nucleus exome sequencing. Genome Biol. *16*, 55. https://doi.org/10.1186/s13059-015-0616-2.
57. Fu, Y., Li, C., Lu, S., Zhou, W., Tang, F., Xie, X.S., and Huang, Y. (2015). Uniform and accurate single-cell sequencing based on emulsion whole-genome amplification. Proc. Natl. Acad. Sci. USA *112*, 11923–11928. https://doi.org/10.1073/pnas.1513988112.
58. Chen, C., Xing, D., Tan, L., Li, H., Zhou, G., Huang, L., and Xie, X.S. (2017). Single-cell whole-genome analyses by Linear Amplification via Transposon Insertion (LIANTI). Science *356*, 189–194. https://doi.org/10.1126/science.aak9787.
59. Zafar, H., Wang, Y., Nakhleh, L., Navin, N., and Chen, K. (2016). Monovar: single-nucleotide variant detection in single cells. Nat. Methods *13*, 505–507. https://doi.org/10.1038/nmeth.3835.
60. Bohrson, C.L., Barton, A.R., Lodato, M.A., Rodin, R.E., Luquette, L.J., Viswanadham, V.V., Gulhan, D.C., Cortés-Ciriano, I., Sherman, M.A., Kwon, M., et al. (2019). Linked-read analysis identifies mutations in single-cell DNA-sequencing data. Nat. Genet. *51*, 749–754. https://doi.org/10.1038/s41588-019-0366-2.
61. Hård, J., Al Hakim, E., Kindblom, M., Björklund, Å.K., Sennblad, B., Demirci, I., Paterlini, M., Reu, P., Borgström, E., Ståhl, P.L., et al. (2019). Conbase: a software for unsupervised discovery of clonal somatic mutations in single cells through read phasing. Genome Biol. *20*, 68. https://doi.org/10.1186/s13059-019-1673-8.
62. Dong, X., Zhang, L., Milholland, B., Lee, M., Maslov, A.Y., Wang, T., and Vijg, J. (2017). Accurate identification of single-nucleotide variants in whole-genome-amplified single cells. Nat. Methods *14*, 491–493. https://doi.org/10.1038/nmeth.4227.
63. McInerney, P., Adams, P., and Hadi, M.Z. (2014). Error Rate Comparison during Polymerase Chain Reaction by DNA Polymerase. Mol. Biol. Int. 287430. https://doi.org/10.1155/2014/287430.
64. Hosokawa, M., Nishikawa, Y., Kogawa, M., and Takeyama, H. (2017). Massively parallel whole genome amplification for single-cell sequencing using droplet microfluidics. Sci. Rep. *7*, 5199. https://doi.org/10.1038/s41598-017-05436-4.
65. Lu, N., Li, J., Bi, C., Guo, J., Tao, Y., Luan, K., Tu, J., and Lu, Z. (2019). ChimeraMiner: An Improved Chimeric Read Detection Pipeline and Its Application in Single Cell Sequencing. Int. J. Mol. Sci. *20*, 1953. https://doi.org/10.3390/ijms20081953.
66. Wang, Y., Waters, J., Leung, M.L., Unruh, A., Roh, W., Shi, X., Chen, K., Scheet, P., Vattathil, S., Liang, H., et al. (2014). Clonal evolution in breast cancer revealed by single nucleus genome sequencing. Nature *512*, 155–160. https://doi.org/10.1038/nature13600.
67. Martin, M. (2011). Cutadapt removes adapter sequences from high-throughput sequencing reads. EMBnet. j. *17*, 10. https://doi.org/10.14806/ej.17.1.200.
68. Li, H. (2013). Aligning sequence reads, clone sequences and assembly contigs with BWA-MEM. Preprint at arXiv. https://doi.org/10.48550/arXiv.1303.3997.
69. McKenna, A., Hanna, M., Banks, E., Sivachenko, A., Cibulskis, K., Kernytsky, A., Garimella, K., Altshuler, D., Gabriel, S., Daly, M., and DePristo, M.A. (2010). The Genome Analysis Toolkit: a MapReduce framework for analyzing next-generation DNA sequencing data. Genome Res. *20*, 1297–1303. https://doi.org/10.1101/gr.107524.110.
70. Li, H., Handsaker, B., Wysoker, A., Fennell, T., Ruan, J., Homer, N., Marth, G., Abecasis, G., and Durbin, R.; 1000 Genome Project Data Processing Subgroup (2009). The Sequence Alignment/Map format and SAMtools. Bioinformatics *25*, 2078–2079. https://doi.org/10.1093/bioinformatics/btp352.
71. Quinlan, A.R., and Hall, I.M. (2010). BEDTools: a flexible suite of utilities for comparing genomic features. Bioinformatics *26*, 841–842. https://doi.org/10.1093/bioinformatics/btq033.
72. Layer, R.M., Chiang, C., Quinlan, A.R., and Hall, I.M. (2014). LUMPY: a probabilistic framework for structural variant discovery. Genome Biol. *15*, R84. https://doi.org/10.1186/gb-2014-15-6-r84.
73. Chiang, C., Layer, R.M., Faust, G.G., Lindberg, M.R., Rose, D.B., Garrison, E.P., Marth, G.T., Quinlan, A.R., and Hall, I.M. (2015). SpeedSeq: ultra-fast personal genome analysis and interpretation. Nat. Methods *12*, 966–968. https://doi.org/10.1038/nmeth.3505.
74. Wickham, H., Averick, M., Bryan, J., Chang, W., McGowan, L., François, R., Grolemund, G., Hayes, A., Henry, L., Hester, J., et al. (2019). Welcome to the tidyverse. J. Open Source Softw. *4*, 1686. https://doi.org/10.21105/joss.01686.
75. Wickham, H. (2016). ggplot2 (Springer International Publishing). https://doi.org/10.1007/978-3-319-24277-4.
76. Gu, Z., Eils, R., and Schlesner, M. (2016). Complex heatmaps reveal patterns and correlations in multidimensional genomic data. Bioinformatics *32*, 2847–2849. https://doi.org/10.1093/bioinformatics/btw313.
77. Leisch, F. (2004). FlexMix: A General Framework for Finite Mixture Models and Latent Class Regression inR. J. Stat. Software *11*, 1–18. https://doi.org/10.18637/jss.v011.i08.
78. R Core Team (2017). R: A Language and Environment for Statistical Computing (R Foundation for Statistical Computing).
79. Cameron, D.L., Di Stefano, L., and Papenfuss, A.T. (2019). Comprehensive evaluation and characterisation of short read general-purpose structural variant calling software. Nat. Commun. *10*, 3240. https://doi.org/10.1038/s41467-019-11146-4.

CellPress
OPEN ACCESS

STAR★METHODS

KEY RESOURCES TABLE

REAGENT or RESOURCE	SOURCE	IDENTIFIER
Chemicals, peptides, and recombinant proteins		
Fibroblast growth medium	Sigma-Aldrich	116-500
DMEM: F12	Lonza	BE04-687Q
IMDM	ATCC	30-2005
Fetal bovine serum	Biochrom	S01005
Penicillin/streptomycin	Lonza	DE17-602E
Hoechst 33342	BD Biosciences	561908
Accutase enzyme	Linus	l0950-100C
Phosphate-buffered saline (PBS)	Lonza	17-513F
Propidium iodide	BD Pharmingen	556463
DNase/RNase free water	ThermoFisher	10977-035
NEBuffer 4 10X	New England Biolabs	174B7004S
MseI 50U/μl	New England Biolabs	R0525M
AMPure XP beads	Agencourt, Beckman Coulter	A63881
Critical commercial assays		
Ampli1	Menarini Silicon Biosystems	WGOO1R
MALBAC	Yikon Genomics	YK001B
PicoPLEX	Rubicon Genomics	R30050
Illustra Single Cell GenomiPhi	GE Healthcare	29-1081-07
REPLI-g Single-Cell	QIAGEN	509150345
TruePrime	SYGNIS	350100
REPLI-g human control kit	QIAGEN	150090
Ampli1 QC kit	Menarini Silicon Biosystems	WGQC4
Ampli1 ReAmp/ds kit	Menarini Silicon Biosystems	WGRDS1
QIAquick PCR Purification	QIAGEN	50928104
dsDNA HS	ThermoFisher Scientific	Q32854
dsDNA BR	ThermoFisher Scientific	Q32853
D5000 assay	Agilent Technologies	5067-5592/5067-5593
Genomic DNA assay	Agilent Technologies	5067-5365/5067-5366
QIAamp DNA Mini kit	QIAGEN	51304
SureSelect^{QXT} Library prep kit	Agilent Technologies	G9682B
NxSeq AmpFREE Low DNA	Lucigen	14000-1
Ion Plus Fragment library	ThermoFisher Scientific	4471252
Nextera DNA sample preparation kit	Illumina	15028211
KAPA Library Preparation kit	Kapa Biosystems	KK8201
NEXTflex-96 DNA Barcodes	Bioo Scientific	514105
High Sensitivity DNA assay	Agilent Technologies	5067-4626
High Sensitivity D1000 assay	Agilent Technologies	5067-5584/5067-5585
Kapa Library Quantification Kit	Kapa Biosystems	KK4824
Ion Library Quantitation Kit	Life Technologies	4468802
Deposited data		
Raw data	This paper	SRA: PRJNA494024

(*Continued on next page*)

Continued

REAGENT or RESOURCE	SOURCE	IDENTIFIER
Human reference genome hs37d5	GATK	https://console.cloud.google.com/storage/browser/gcp-public-data–broad-references/Homo_sapiens_assembly19_1000genomes_decoy
Experimental models: Cell lines		
Human: HDF neonatal	Sigma-Aldrich	106-05N
Human: Caco-2	ATCC	HTB-37
Human: Z-138	ATCC	CRL-3001
Software and algorithms		
FACSDiva (v.8.0.1)	BD Biosciences	https://www.bdbiosciences.com/
FlowJo (v7.6.2)	FlowJo, LLC	https://www.flowjo.com/
CutAdapt (v.1.11, v.1.14, v.1.18)	Martin[67]	https://cutadapt.readthedocs.io/en/stable/
BWA-MEM (v.0.7.15-r1140, v.0.7.17)	Li[68]	https://github.com/lh3/bwa/
Torrent Mapping Alignment Program (TMAP; v.3.4.1)	Thermo Fisher Scientific	https://github.com/iontorrent/TMAP/
Picard (v.2.2.1, v.2.18.14) *SortSam MarkDuplicates SamToFastq DownsampleSam*	Broad Institute	http://broadinstitute.github.io/picard/
GATK (v.3.7, v.4.0.0.0) *HaplotypeCaller VariantRecalibration SelectVariants GenotypeGVCF ApplyVQSR*	McKenna et al.[69]	https://github.com/broadinstitute/gatk/releases
Samtools (v.1.9) *flagstats bedcov mpileup depth*	Li et al.[70]	https://www.htslib.org/download/
Bedtools (v.2.29.0) genomecov *makewindows nuc*	Quinlan and Hall[71]	https://bedtools.readthedocs.io/en/latest/content/installation.html
Pysamstats (v.1.1.2)	N/A	https://github.com/alimanfoo/pysamstats
LUMPY (v.0.2.13)	Layer et al.[72]	https://github.com/arq5x/lumpy-sv
svtyper (v.0.7.0)	Chiang et al.[73]	https://github.com/hall-lab/svtyper
R (v.4.4.1)	N/A	https://www.r-project.org/
R package reshape2 (v.1.4.4)	N/A	https://github.com/hadley/reshape
R package dplyr (v.1.1.4)	Wickham et al.[74]	https://github.com/tidyverse/dplyr
R package ggplot2 (v.3.5.1)	Wickham[75]	https://github.com/tidyverse/ggplot2
R package data.table (v.1.15.4)	N/A	https://github.com/Rdatatable/data.table
R package ggpubr (v.0.6.0)	N/A	https://rpkgs.datanovia.com/ggpubr/
R package extrafont (v.0.19)	N/A	https://github.com/wch/extrafont
R package Hmisc (v.5.2.0)	N/A	https://hbiostat.org/R/Hmisc/
R package RColorBrewer (v.1.1.3)	N/A	https://github.com/cran/RColorBrewer
R package corrplot (v.0.95)	N/A	https://github.com/taiyun/corrplot
R package ggnewscale (v.0.5.0)	N/A	https://github.com/eliocamp/ggnewscale
R package plyr (v.1.8.9)	N/A	https://github.com/hadley/plyr
R package scales (v.1.3.0)	N/A	https://github.com/r-lib/scales
R package ComplexHeatmap (v.2.20.0)	Gu et al.[76]	https://github.com/jokergoo/ComplexHeatmap
R package tidyr (v.1.3.1)	Wickham et al.[74]	https://github.com/tidyverse/tidyr
Other		
Scripts for the bioinformatic analysis	This paper	https://doi.org/10.5281/zenodo.15025379; https://gitlab.com/phylocancer/scwga-benchmark/

EXPERIMENTAL MODEL AND STUDY PARTICIPANT DETAILS

Cell lines

We used three different cell lines: HDF, Caco-2, and Z-138. HDF is a healthy neonatal, diploid fibroblast cell line (HDF) purchased from Sigma-Aldrich (https://www.sigmaaldrich.com); Caco-2 is a polyploid colorectal cancer cell line with a modal chromosome number of 96 purchased from the American Type Culture Collection (ATCC; https://www.atcc.org); Z-138 is a hyperdiploid mantle cell lymphoma cell line with a modal chromosome number of 49, purchased from ATCC. We cultured all cell lines under an

atmosphere containing 5% CO_2 at 37°C. We grew HDF in an all-in-one ready-to-use fibroblast growth media (Sigma-Aldrich), Caco-2 in a media consisting of Dulbecco's Modified Eagle's Medium/F12 with 3.151 g/l glucose and L-glutamine (Lonza) and Z-138 with Iscove's Modified Dulbecco's Medium (ATCC). For Caco-2 and Z-138, we completed the media with 10% fetal bovine serum EU standard (Biochrom) and 1% penicillin/streptomycin (Lonza) at a working concentration of 100 units of potassium penicillin and 100 μg of streptomycin sulfate per 1 ml of culture media.

METHOD DETAILS

Single-cell isolation

Following the fabricant's recommendations, we cultured HDF and Caco-2 cells until 80% confluence before staining with Hoechst 33342 (BD Biosciences). After that, we harvested the cells using the accutase enzyme (not needed for Z-138), resuspended them at a concentration of 10^6 cells per ml in phosphate-buffered saline (PBS), filtered using a 70 μm cell strainer and marked them with propidium iodide (PI; BD Pharmingen). Then, we sorted alive single cells in G0/G1 with a BD Biosciences FACSAria III flow cytometer (BD Biosciences, Madrid, Spain) and collected them into 96-well plates with 1-3 μl of PBS (Figure S7). For sorting, we used BD FACSDiva v8.0.1 (BD Biosciences, Madrid, Spain) and FlowJo v7.6.2 (FlowJo, LLC, Ashland, OR, USA) for further analysis. For Z-138, we followed the same strategy but without Hoechst staining and using a FACS Aria 2.0 (BD Biosciences, Madrid, Spain) for sorting. We stored the single cells at -80°C until they were ready for amplification.

Single-cell whole-genome amplification (scWGA)

We used six different kits for amplification: Ampli1 (Menarini Silicon Biosystems), Multiple Annealing and Looping Based Amplification Cycles (MALBAC; Yikon Genomics), PicoPLEX (Rubicon Genomics), Illustra Single Cell GenomiPhi (GE Healthcare), REPLI-g Single-Cell (QIAGEN) and TruePrime (SYGNIS) following the manufacturer's protocols (Figure S1B; Table S2). To limit contamination, we carried out scWGA in a laminar-flow hood using a dedicated set of pipettes and UV-irradiated plastic materials. We also included positive (10 ng/μl REPLI-g human control kit, QIAGEN) and negative (DNase/RNase free water) controls. For Ampli1, we carried a few extra steps after amplification. We used the Ampli1 QC kit to select positive amplification products for four PCR markers. To increase the total dsDNA content, we used the Ampli1 ReAmp/ds kit. Afterward, we removed the adaptors adding 5 μl of NEBuffer 4 10X (New England Biolabs), 1 μl of MseI 50U/μl (New England Biolabs), and 19 μl of nuclease-free water to 25 μl of dsDNA, using a thermal cycler at 37°C for 3 h, followed by enzyme inactivation at 65°C for 20 min.

Attending the fabricant's recommendations, we purified the PicoPLEX and MALBAC products with the QIAquick PCR Purification protocol (QIAGEN) and the Ampli1 products with 1.8X AMPure XP beads (Agencourt, Beckman Coulter). MDA methods do not include a purification step. We measured DNA yield with the dsDNA HS or BR assay in a Qubit 3.0 (ThermoFisher Scientific) fluorometer and amplicon fragment size with a 2200 TapeStation platform (Agilent Technologies). We measured the amplicons from the non-MDA-based scWGA methods using the D5000 ScreenTape System and the amplicons from the MDA-based kits using the Genomic DNA ScreenTape System. The latter also allowed us to measure the integrity of the amplicons (DNA Integrity Number or DIN).

We amplified >570 cells but finally selected the best 230 cells regarding DNA quantity and quality. We amplified 34 cells with Ampli1 (4 HDF, 12 Caco-2, and 18 Z-138), 40 with MALBAC (4 HDF, 18 Caco-2, and 18 Z-138), 40 with PicoPLEX (4 HDF, 18 Caco-2 and 18 Z-138), 37 with GenomiPhi (4 HDF, 18 Caco-2 and 15 Z-138), 35 with REPLI-g (4 HDF, 16 Caco-2 and 15 Z-138) and 44 with TruePrime (4 HDF, 22 Caco-2 and 18 Z-138) (Figure S2; Table S2).

Bulk DNA extraction

According to the fabricant's recommendations, we extracted bulk genomic DNA (gDNA) from the HDF cell line with the QIAamp DNA Mini kit (QIAGEN). We estimated concentration and gDNA integrity as previously described for the amplified products from single cells.

Next-generation sequencing libraries

We built 230 single-cell whole-genome libraries employing five different library preparation kits: SureSelectQXT (Agilent Technologies), NxSeq AmpFREE Low DNA (Lucigen), Ion Plus Fragment library (ThermoFisher Scientific), Nextera DNA (Illumina), and KAPA (Kapa Biosystems). We built SureSelect and NxSeq libraries following the commercial indications while slightly modifying the Ion Plus and Nextera protocols. KAPA libraries were built using a modified protocol at the sequencing facility of the National Center for Genomic Analysis (CNAG; http://www.cnag.crg.eu) (Table S3). We mechanically sheared the DNA in an S2 or a LE220 Focused-ultrasonicator (Covaris) for the NxSeq, Ion Plus, and KAPA protocols (Table S6), while for SureSelect and Nextera, we fragmented the DNA enzymatically. For Ion Plus, we included an extra purification step with AMPure XP beads (1.2X beads/sample ratio) (Agencourt, Beckman Coulter) to better remove NGS adaptors. For Nextera, we used 200 μl of washing buffer instead of the 300 μl recommended by the provider, the centrifugation speed was 10,000 g at room temperature (RT) for 30 s instead of 1,300 g at 20°C for 2 min, and we used AMPure XP beads in a 0.8X ratio instead of 0.6X. In addition, we eluted the Nextera libraries in 20 μl of resuspension buffer instead of 32.5 μl after a 5 min air-dried step instead of 15 min. For the modified KAPA protocol, we performed the end-repair of 500 ng of sheared DNA, adenylation, and ligation to Illumina-specific indexed paired-end adaptors (NEXTflex-96 DNA Barcodes, Bioo Scientific). We selected the DNA by size in two steps (0.65X and 0.85X beads/sample ratio) with AMPure XP

beads to reach the desired fragment size (450 bp). Finally, we measured the library insert sizes with a 2100 Bioanalyzer High Sensitivity DNA Kit or a 2200 TapeStation High Sensitivity D1000 assay. We quantified library concentration with the Kapa Library Quantification Kit (Kapa Biosystems) in the case of Illumina and with the Ion Library Quantitation Kit (Life Technologies) for Ion Torrent.

In addition, we constructed a whole-genome HDF bulk library using NxSeq AmpFREE Low DNA (Lucigen) (Table S3). We performed size selection using AMPure XP beads and checked fragment size with the 2100 Bioanalyzer High Sensitivity DNA Kit. Finally, we quantified library concentration using the KAPA Library Quantification Kit.

Whole-genome sequencing

We initially sequenced all the single-cell libraries at shallow depth (0.07–1.76X). We sequenced 24 HDF and 166 Caco-2/Z-138 libraries on an Illumina HiSeq 4000 (PE150) or HiSeq 2000 (PE125), respectively, at CNAG. We sequenced the remaining 40 libraries with an Ion Proton platform (Ion PI chip v3) at the Galician Public Foundation of Genomic Medicine (FPGMX; http://www.xenomica.eu). We also sequenced the bulk library of HDF at 30X on an Illumina HiSeq 4000 (PE150) at CNAG. In addition, for the 24 HDF libraries, we completed a second WGS run at a higher depth (7.6-16.8X) on a HiSeq 2500 v4 (PE125) at CNAG.

Preprocessing of NGS data

From Illumina data, we clipped library adapters and those included in the Ampli1, PicoPLEX, and MALBAC amplifications using CutAdapt (v.1.11, v.1.14, v.1.18).[67] We mapped the sequencing reads with at least 70 bp to the human reference genome (hs37d5) with BWA-MEM (v.0.7.15-r1140, v.0.7.17).[68] We sorted reads and flagged duplicates with Picard *SortSam* (v.2.2.1, v.2.18.14; http://broadinstitute.github.io/picard) and Picard *MarkDuplicates*, respectively. We independently mapped reads from different lanes and merged them during the duplicate marking process, considering their read group. Regarding Ion Plus libraries, to map the reads with the Torrent Mapping Alignment Program (TMAP; v.3.4.1; https://github.com/iontorrent/TMAP) to the hs37d5 genome, we had to transform first of all the original BAM files to FASTQ format using Picard *SamToFastq*. We also sorted the BAM files and marked duplicates as explained above.

To carry out the variant calling at similar sequencing depths for all the HDF cells and avoid potential batch effects, we downsampled the corresponding BAM files at 7.6X (the lowest depth observed) using Picard *DownsampleSam*. Also, we recalibrated the HDF base quality scores using GATK (v.3.7).[69] Afterward, we realigned the reads from the single cells and the bulk around known indels to avoid potential false SNV calls unrelated to the amplification process but due to misalignments.

Mapping rates and duplicates

To calculate the percentage of mapped reads and duplicates, we analyzed the BAM files with the duplicate flags annotated using Samtools (v.1.9) *flagstats*.[70] To obtain the mapping rate, we divided the mapped alignments by the total number of alignments, whereas to calculate the duplication rates, we divided the number of duplicate alignments by the number of mapped alignments.

Genome breadth

We calculated the percentage of autosomes and sex chromosomes covered by one or more reads (i.e., genome breadth) using Bedtools (v.2.29.0)[71] *genomecov*. For this calculation, we downsampled all single-cell and bulk BAM files to the same depth (0.15X) with Picard *DownsampleSam* (with the options *HighAccuracy* for the single cells and *ConstantMemory* for the bulk). We discarded 12 cells with less than 0.15X. In addition, for HDF, we computed the genome breadth at 7.6X. We then merged all four downsampled bam files at 7.6X for each scWGA kit, to create "pseudobulks" and measured genome breadth as previously described.

Amplification disuniformity

We estimated amplification disuniformity using the downsampled BAM files at 0.15X. We defined non-overlapping 100-kb windows along the genome using Bedtools *makewindows* and counted the number of reads mapped within each window with Samtools *bedcov*. Then, we calculated the Kullback-Leibler (K-L) divergence between the read count distribution of every cell and the bulk using the R *FlexMix* package.[77] We then used the resulting value to measure amplification disuniformity: the lower the K-L divergence to the bulk, the lower the amplification disuniformity.

Amplification recurrence

To understand whether a given scWGA method tends to preferentially amplify the same genomic regions in different cells compared to other scWGA methods, we counted the number of reads within non-overlapping windows of 1 Mb with Pysamstats (v.1.1.2) (https://github.com/alimanfoo/pysamstats). For this, we used BAM files at 7.6X –after removing duplicates, secondary alignments, and unmapped reads with Samtools *view*– as input. Subsequently, we computed the Pearson correlation coefficient of the read counts between pairs of single cells (amplified with the same scWGA kit or not) and between single cell and bulk. We further explored the correlations between read counts and GC content in sliding windows. We measured the GC content with Bedtools *nuc*.

Allelic imbalance, ADO, and LDO

During scWGA, the two alleles of a diploid cell can be unequally amplified. Deviations of allele frequencies at heterozygous germline sites reveal such events. If these frequencies differ from the theoretical 50%, we consider it an allelic imbalance event. If the

imbalance is so high that one of the alleles is completely lost and cannot be detected, we designate it as allelic dropout or ADO. Finally, if both alleles are lost, we define this event as locus dropout or LDO (Figure S1A). To calculate the allele frequencies at the heterozygous germline sites, we used the 7.6X HDF dataset. Besides, we limited the analysis to the autosomes since they are primarily diploid.

Allelic imbalance

We ran GATK *HaplotypeCaller* for the HDF bulk with the parameter –pcr_indel_model set to NONE. We ran GATK *VariantRecalibration* and *ApplyVQSR* (v. 4.0.0.0) to select a high-confidence set of variants (-ts-filter-level 90.0), and then we used GATK *SelectVariants* to keep the heterozygous sites. In parallel, we created pileup files from all the HDF single cells and bulk with Samtools *mpileup* and extracted the alternative allele fraction at the high-confidence heterozygous positions using a Python script. We only considered the allele frequencies derived from sites covered by at least 15 reads. To obtain a smooth distribution from the discrete counts, we estimated the probability density function of the alternative allele fractions with the *core* R stats package,[78] with the *bandwidth adjust* parameter set to three.

Allelic dropout (ADO) and locus dropout (LDO)

To measure ADO, we need to obtain the genotypes for the bulk and the single cells. For this, we ran GATK *HaplotypeCaller* in -ERC GVCF mode for every single cell and the bulk independently (again setting –pcr_indel_model to NONE). Then, we merged the resulting gVCFs with GATK *GenotypeGVCF,* combining the calls for every cell with the calls obtained for the bulk, keeping the invariable positions. We counted an ADO event when the bulk was called heterozygous (AB) and the single cell homozygous for either the reference or the alternative allele (AA or BB) (Figure S4B). We only considered positions covered by 15 or more reads in both single cells and bulk. The exact calculation per cell was

$$ADO\ rate = \frac{1}{N_{het}} \sum_{i=1}^{N_{het}} \alpha \quad \begin{cases} \alpha = 1 & if\ gSC_i \neq gB_i \\ \alpha = 0 & otherwise \end{cases}, \qquad \text{(Equation 1)}$$

where N_{het} is the number of heterozygous positions in the bulk, i is the considered genomic position, gSC_i is the genotype of the single cell at position i, and gB_i is the genotype of the bulk at position i.

Locus dropout (LDO). Using the genotypes obtained above, we counted an LDO event when the bulk was genotyped as AB, and the genotype was not called in the single cell (./. or NA), independently of the coverage at that position. The exact calculation per cell was

$$LDO\ rate = \frac{1}{N_{het}} \sum_{i=1}^{N_{het}} \alpha \quad \begin{cases} \alpha = 1 & if\ gSC_i = NA\ and\ gB_i = AB \\ \alpha = 0 & otherwise \end{cases}. \qquad \text{(Equation 2)}$$

Amplification polymerase errors

During the whole-genome amplification, polymerases can introduce errors like incorrect bases, insertions, and deletions. These errors become part of the sequenced templates and appear as reads carrying out distinct alleles. These wrong reads can lead to spurious SNV and indel calls.

Erroneous bases

We calculated the proportion of alternative alleles in the single-cell reads at those positions genotyped as 0/0 in the bulk. We only considered bulk sites covered by at least 20 reads with a reference allele and zero reads with an alternative.

False SNVs

Using the same genotypes estimated above for the ADO calculation, we counted a false SNV call event when the bulk genotype was homozygous, and the single cell had a different genotype than the bulk (Figure S4B). We only considered autosomal positions with 15 or more reads in both single cells and bulk. The exact calculation per cell was

$$False\ SNV\ rate = \frac{1}{N_{hom}} \sum_{i=1}^{N_{hom}} \alpha \quad \begin{cases} \alpha = 1 & if\ gSC_i \neq gB_i \\ \alpha = 0 & otherwise \end{cases}. \qquad \text{(Equation 3)}$$

We also explored the error profile of the false SNV calls directly, extracting the alternative and reference alleles from the VCFs and grouping them into different categories.

False indel rate

Using the same VCFs as for the false SNV calls, we identified indels with GATK *SelectVariants* and calculated the number of false and true positives and negatives (FP, TP, FN, and TN) only in autosomes as follows:

FP: 0/0 for the bulk, and 0/1 or 1/1 in the single cell
FN: 0/1 or 1/1 for the bulk, and 0/0 in the single cell
TP: 0/1 or 1/1 for the bulk, and 0/1 or 1/1 in the single cell
TN: 0/0 for the bulk and 0/0 in the single cell

Then, we computed *sensitivity* as 100×TP/(TP + FN) and *specificity* as 100×TN/(TN + FP).

Copy number

The uneven distribution of the coverage, added to the possibility of ADO, can make copy number (CN) detection from a single cell very problematic. We compared how different scWGA methods behave in this regard using the coverage dispersion measure (MAD).[45] For this calculation, we used the downsampled BAM files at the lowest depth for each cell line (0.25X, 0.07X, and 0.08X for HDF, Caco-2, and Z-138, respectively). We filtered out reads with a mapping quality lower than 20 from the downsampled BAMs using Samtools and created the BED files required to run Ginkgo[45] with Bedtools. We ran Ginkgo under default settings except for the Binning Simulation Options, which were set to 150 bp reads and mapping with BWA. The segmentation was inferred independently for each sample to allow a fair comparison. We calculated the MAD from the resulting read counts using a custom R script. Besides, we also segmented the 24 HDF single cells and the bulk using all the other possible bin segmentation sizes allowed by Ginkgo. For each bin size, we computed the CN distance from every cell to the bulk, which is defined as the total length of the genomic segments with different copy numbers divided by the length of the CN profile. To compute sensitivity and specificity as before, we obtained the counts for FP, FN, TP, and TN for autosomes as follows (for sex chromosomes, exchange 1 for 2):

FP: CN of 2 for the bulk, and CN $\neq$ 2 in the single cell
FN: CN $\neq$ 2 for the bulk, and CN = 2 in the single cell
TP: CN $\neq$ 2 for the bulk, and CN $\neq$ 2 in the single cell
TN: CN of 2 for the bulk, and CN = 2 in the single cell

Structural variant breakpoints

We identified structural variants in the HDF 7.6X data. For this, we ran LUMPY (v.0.2.13)[72] independently for each single cell and the bulk, and then we genotyped the calls using svtyper (v.0.7.0).[73] We selected the autosomal breakpoints with genotypes 0/1, 1/0, or 1/1 and obtained the depth in those positions for all the samples using Samtools *depth*. We removed breakpoints in positions covered by less than 15 reads in the bulk of the single cell. We also removed breakpoints with abnormally high depth in the bulk (>1,000X) since they tend to be errors.[79] We considered the positions with no called breakpoint to be genotype 0/0. Then, we compared the breakpoints in the single cells and in the bulk to count FP, FN, and TP in the same way we did for indels. As the LUMPY output does not contain the TN, we calculated them by getting the number of autosomal positions showing at least 15 reads in both bulk and single cells using Samtools *mpileup* and subtracting the number of FP, FN, and TP from this value. Then, we computed sensitivity and specificity as described above.

QUANTIFICATION AND STATISTICAL ANALYSIS

We performed the downstream data analysis in R using the tidyverse[74] framework. We calculated standard descriptive statistics using the *kruskal.test*, *wilcox.test*, and *cor.test* functions available in the *core* R stats package[78] and produced the plots using ggplot2,[75] and ComplexHeatmap[76] R packages.